**ORIGINAL ARTICLE**

# Discovery of new code interference phenomenon in GPS observables

Connor D. Flynn[1] · Anthony M. McCaffrey[1] · P. T. Jayachandran[1] · Richard B. Langley[2]

## Abstract

The Global Positioning System (GPS) provides satellite-based navigation signals, which are employed in many fields, including agriculture, transportation, aviation, and military/personal navigation. In an effort to minimize interference among GPS satellites and to enable GPS receivers to discern satellite identity, each satellite is assigned a specific pseudorandom noise (PRN) sequence that is used to modulate the phase of the corresponding signal. The codes that modulate the current GPS landscape are constructed in such a way that cross-correlation among codes is kept to a bounded minimum, which should significantly limit harmful signal interference. In this study, the efficacy of the current PRN-based modulation system is called into question as GPS signal amplitude and carrier phase data over the past decade show frequent interference between satellite signals.

**Keywords** GPS · Interference · Frequency spectrum analysis · Ionospheric scintillation

## Introduction

Global Positioning System (GPS) navigation signals have numerous applications in research, industry, and everyday life. GPS is one of several global navigation satellite systems, which include the Russian Global Navigation Satellite System (GLONASS), the European Galileo, and the Chinese BeiDou systems. While each of these systems differ in design, all are similar at a fundamental level in that they record a set of observables, which provide information on signal phase, amplitude, and Doppler frequency offset, among others. Using the available GPS observables, it is possible to acquire navigation data and deduce information pertaining to signal efficacy at the receiver, satellite, or along the ray path in between. Of particular interest in this intermediary region is the ionosphere—a significantly ionized portion of the upper atmosphere—whose dynamic nature can lead to large-scale disruptions in radio wave propagation (Budden 1985). One such ionospheric phenomenon, known as scintillation, results in irregular fluctuations in the amplitude and phase of a radio wave as it passes through regions of irregular electron density (Crane 1977; Wernik et al. 2003). Scintillation can result in the temporary loss of satellite lock, which can significantly constrain the accuracy of, or even prevent, receiver positioning (Langley 1996; Doherty et al. 2003; SBAS-IONO 2012). Through research into methods of mitigating and forecasting these ionospheric events, experts aim to overcome this interference and increase both the accuracy and reliability of GPS positioning.

While the effects of the ionosphere on GPS signals are not without importance, ground-based interference can impact GPS operation just as significantly. Multipath refers to a mode of GPS interference whereby radio waves reach a receiver by multiple interfering paths, usually through reflection by nearby objects; thus, multipath is an especially predominant problem in regions of dense surroundings such as forests or cities (Langley 1996; Soubielle et al. 2002). Since sources of multipath are typically stationary with respect to a fixed receiver, disturbances in phase, amplitude, and pseudorange data due to such objects are often repeated every sidereal day and can thus be identified with a sidereal-repetition filter (Ragheb et al. 2007). Significant research has already been (Tamazin et al. 2016), and continues to be, carried out on ways to mitigate multipath in real time for application in GPS-based devices.

✉ Connor D. Flynn
connor.flynn@unb.ca

[1] Department of Physics, University of New Brunswick, 8 Bailey Drive, Fredericton E3B 5A3, Canada

[2] Department of Geodesy and Geomatics Engineering, University of New Brunswick, 15 Dineen Drive, Fredericton E3B 5A3, Canada

The need for satellite navigation systems to provide accurate and precise data for both civilian and military use has led to substantial research into the identification and mitigation of GNSS interference; as such, the identification of novel sources of interference holds great potential for future improvements to GPS-based research and navigation. One potential source of GPS interference involves the satellite signals themselves, whereby individual received signals overlap and interfere with one another; however, the current GPS constellation has safeguards in place to minimize such interference (Spilker 1996). GPS operates on a code division multiple access (CDMA) basis, whereby all satellites transmit code-modulated signals at the same specific carrier frequencies. The main carrier frequency used by GPS is L1 (1575.42 MHz). The L1 carrier waves are modulated with a satellite-specific pseudorandom noise (PRN) sequence—a set of binary values that appear stochastic and whose cross-correlations are kept to a bounded minimum (Gold 1967; Langley 1996). The apparent randomness of a PRN sequence allows a modulated signal to mimic noise, concealing the signal, and the constrained cross-correlation reduces the possibility of signal misinterpretation (Langley 1996). PRN sequences are replicated at the receiver-level and used to demodulate received signals, allowing for satellite identification without fear of significant signal interference. While the current PRN modulation system has appeared sound to date, with respect to reducing signal interference, the results of this study question the integrity of said modulation and its overall ability to minimize interference.

In this study, we present experimental evidence of GPS signal code interference that has occurred persistently throughout the last decade. By identifying and characterizing the interference, we hope to stimulate research towards improving the overall efficacy of GPS signals for use in both research and industry.

## Data, methods of analysis, and results

All data used in this study was obtained through the recently expanded Canadian High Arctic Ionospheric Network (CHAIN) (Jayachandran et al. 2009) (Fig. 1), which provides high-rate amplitude and phase data sampled at 50 or 100 Hz from 25 receivers located throughout the Canadian North. The receivers include both the NovAtel GSV4004B (Van Dierendonck and Arbesser-Rastburg 2004), capable of providing 50 Hz data, and the Septentrio PolaRxS Pro (McCaffrey and Jayachandran 2017), capable of providing data at 50 or 100 Hz.

GPS observables of interest in this study include signal amplitude, carrier phase, and Doppler frequency offset. While all three observables are provided directly from the PolaRxS, the GSV4004B Doppler offset was obtained as
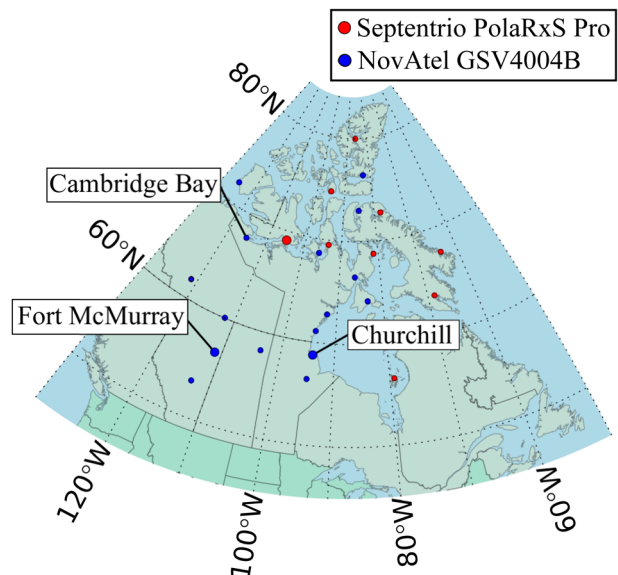


**Fig. 1** CHAIN stations located throughout the Canadian North. The stations whose data are included in this study are labelled

the time derivative of the carrier phase (Simsky and Boon 2003). Relative Doppler ($f_{RD}$) between satellites was calculated as the difference between each of their respective Doppler offsets ($f_{Doppler}$), according to equation

$$f_{RD} = \left| f_{Doppler1} - f_{Doppler2} \right| \tag{1}$$

The relative Doppler served as an indicator of how close satellite reception frequencies were to one another.

Both amplitude and phase data were de-trended using a sixth-order Butterworth high-pass filter with a cut-off frequency of 0.1 Hz (Fremouw et al. 1978). Fourier analysis of observables was performed using the fast Fourier transform (FFT) over 60-s intervals to ensure a small enough timescale to prevent frequency masking and a large enough timescale for adequate resolution in the frequency domain.

Dominant or peak frequencies in the FFT spectrum were defined as those frequencies, above a defined cut-off frequency, that showed a significantly higher-than-expected contribution. The cut-off frequency helped eliminate any low-frequency trends. Thresholds were established to isolate significant peak frequencies by selecting peaks that exceed mean + $n$SD, where SD is standard deviation and $n$ varies depending on the event, with a minimum of 2. Once anomalies in the frequency domain were identified, a more robust analysis was performed.

### Irregularities identified in GPS-derived data

The amplitude and phase of L1 GPS signals received at Churchill station (58.75°N, 265.91°E) at a sampling rate of

**Fig. 2** Eight-minute period of phase (**a**–**c**) and amplitude (**d**–**f**) data obtained from Churchill, Manitoba on May 11, 2015, within 06:00–07:00 UTC for PRN 5, showing de-trended raw data (**a**, **d**), frequency spectrum (**b**, **e**), and raw data restricted to the 2.5–12.5 Hz range (**c**, **f**). Blue and red lines indicate the cut-off frequency and statistical threshold, respectively
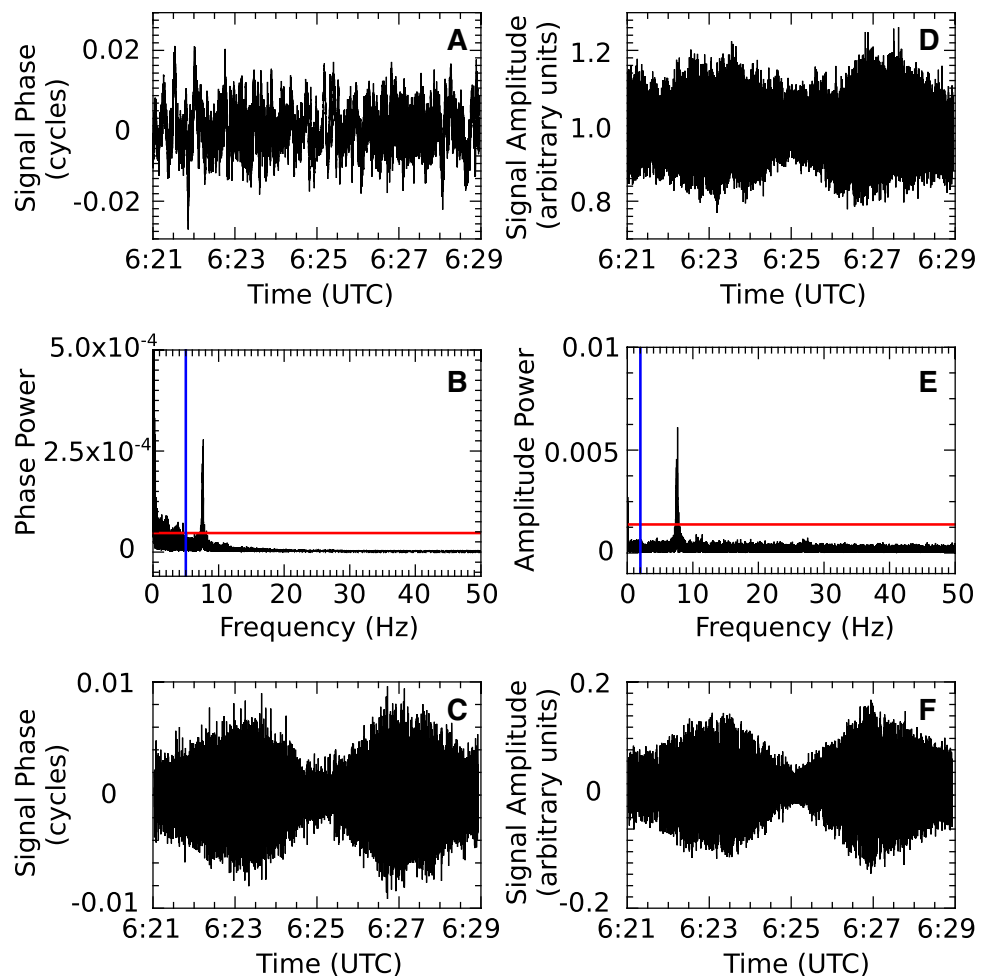
100 Hz by the Septentrio PolaRxS receiver were studied in depth for possible irregularities. Fourier analysis revealed a dominant frequency of approximately 7.5 Hz (Fig. 2b, e) associated with both de-trended phase (Fig. 2a) and amplitude (Fig. 2d) for PRN 5 on May 11, 2015, from 6:21 to 6:29 UTC. Using a digital band-pass filter, the de-trended data in the 2.5–12.5 Hz range was isolated (Fig. 2c, f) to better observe the manifestation of the 7.5 Hz frequency in the time domain within a $\pm 5$ Hz margin of variation. When restricted in the frequency domain, both phase and amplitude data show a nearly identical symmetrical beat-like pattern, corresponding to the dominant 7.5 Hz frequency. A nearly identical peak frequency and corresponding beat pattern were also observed in data from PRN 20 during the same time period. Expanding the analysis to include all CHAIN receivers, distinct frequency peaks were observed on both PRN 5 and PRN 20 for 18 out of 19 stations for which data was available at the given time, including both Septentrio PolaRxS Pro and NovAtel GSV4004B receivers. While the peak frequency is similar in value between observables at a given station and between PRN 5 and PRN 20 at a given station, the peak-frequency value differs between stations.

While the peak frequency shown in Fig. 2 appears stationary over the 8-min period for which it is shown, in reality, the dominant frequency changes significantly over time. Figure 3 shows the wavelet-derived (Daubechies 1990) frequency contour restricted to within 1–15 Hz for the hour surrounding the peak in Fig. 2, during which the observed peak frequency appears intermittently and changes with time. The sky plot of the visible satellites above Churchill shows the relative satellite positioning throughout the hour in question (Fig. 3, bottom), during which PRN 5 and PRN 20 remain relatively close.

Expansion of the analysis to include multiple receivers identified a multitude of similar peak-frequency irregularities dating as far back as the available data goes (2008) and as recently as this paper (2018). The peak-frequency events were observed on all GPS satellites on receivers distributed throughout the Canadian North. The identified events all involved a specific peak frequency simultaneously observed in both amplitude and phase data from at least two satellites at a given receiver. Observed peak frequencies ranged from near-zero Hz to the Nyquist frequency (50 Hz for 100 Hz data and 25 Hz for 50 Hz data), occurring indiscriminately
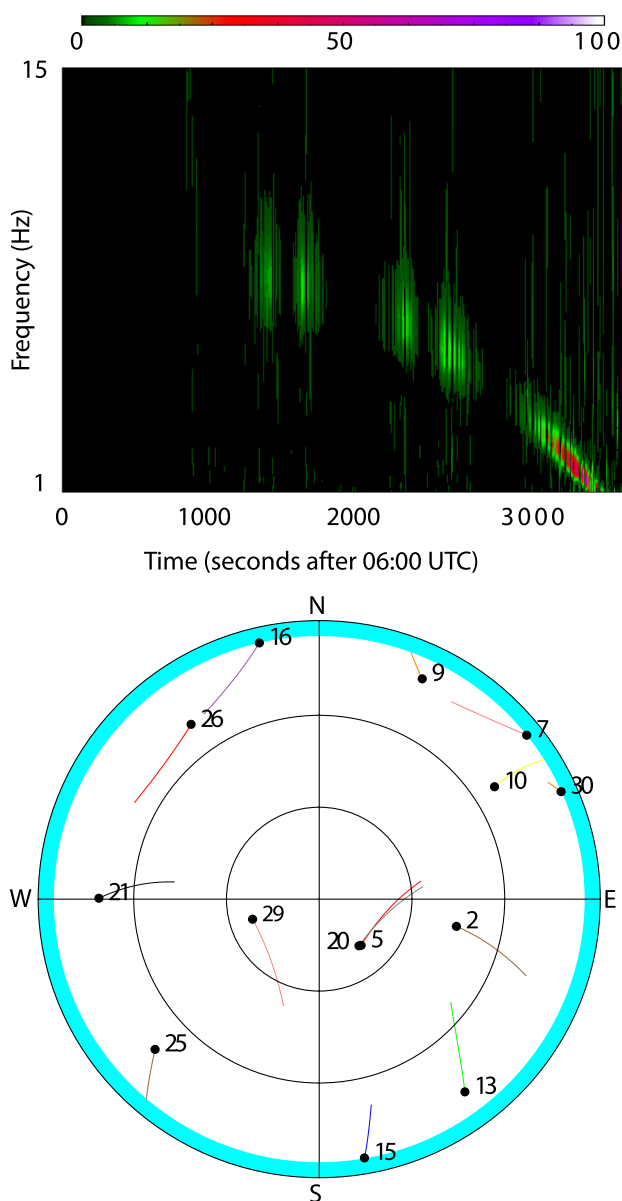
**Fig. 3** Concerning data obtained in Churchill, Manitoba, on May 11, 2015, from 06:00 to 07:00 UTC, presented is (top) the wavelet-derived frequency contour for signal amplitude from PRN 5 showing scaled frequency intensity and (bottom) the sky above Churchill, showing the movement of satellites

at every value in between. While the example featured in Figs. 2 and 3 involved satellites in close proximity to one another, this was not observed to be a requirement for the peak-frequency irregularity; similar peak-frequency events occurred between satellites at variable elevation and azimuthal angles. Similar peak frequencies and beat patterns also often repeated day after day (about 24 h) within the same set of satellites, but showed no consistent time offset due to the intermittent nature of the data.

While the previous example was obtained on a Septentrio PolaRxS receiver at 100 Hz, similar peak-frequency irregularities were also observed on the NovAtel GSV4004B receiver at 50 Hz. Figure 4 shows another peak frequency of approximately 7 Hz (Fig. 4b, e) on January 3, 2009, from 23:34 to 23:66 UTC for PRN 3 at Cambridge Bay station (69.10°N, 254.88°E) for both de-trended phase (Fig. 4a) and amplitude (Fig. 4d). Similar peak frequencies and beat patterns were observed for PRN 26. Unlike the first example, the de-trended data, restricted to 4–9 Hz (Fig. 4c, f)—a $\pm 2.5$ Hz margin of variation, does not clearly show the beat-like pattern as the peak frequency is changing too quickly to produce a discernible pattern.

### Relative Doppler matches observed frequencies

The relative Doppler between satellites involved in the peak-frequency events was calculated. Obtained relative Doppler values showed near-perfect similarity (correlation coefficient ($R$) $> 0.99$) to the observed frequency peaks at similar timescales during the described events. If relative Doppler values exceeded the Nyquist limit of 50 Hz for 100 Hz data (or 25 Hz with 50 Hz data), the frequency was aliased down to its corresponding value. Figure 5 shows the relative Doppler for PRN 5 and 20 (black solid line) and observed statistically significant peak frequencies over 60-s intervals (orange diamonds) for amplitude and phase data from both the Churchill station and the Fort McMurray station (56.64°N, 248.77°E) on May 11, 2015, from 06:00 to 07:00 UTC. It should also be mentioned that the amplitude plot for Churchill contains three observed frequency peaks that do not line up with the relative Doppler. While at first these deviating frequencies may appear as outliers, they actually coincide with the relative Doppler of PRN 5 and PRN 29 in a separate peak-frequency event as identical peaks are observed on both satellites. Several other peak-frequency events involving more than two satellites were observed, though they occur much less frequently than two-satellite events.

Statistical comparison of the observed frequency peaks and relative Doppler was performed by linear correlation. Relative Doppler between interfering satellites was averaged over 60-s intervals to match the timescale over which the observed frequency peaks were recorded. The obtained correlation coefficients for the example outlined in Fig. 5 show a high degree of correlation, with correlation coefficients of 0.9998 (amplitude) and 0.9996 (phase) for Churchill and 0.9996 (amplitude) and 0.9998 (phase) for Fort McMurray (Fig. 5) with linear fits of $y = 1.014x - 0.07510$ (amplitude) and $y = 0.9905x + 0.06891$ (phase) for Churchill and $y = 1.001x - 0.04490$ (amplitude) and $y = 0.9976x + 0.02384$ (phase) for Fort McMurray.

**Fig. 4** Five-minute period of phase (**a**–**c**) and amplitude (**d**–**f**) data obtained from Cambridge Bay, Nunavut, on January 3, 2009, within 23:00–24:00 UTC for PRN 3, showing de-trended raw data (**a**, **d**), frequency spectrum (**b**, **e**), and raw data restricted to the 4–9 Hz range (**c**, **f**). Blue and red lines indicate the cut-off frequency and statistical threshold, respectively
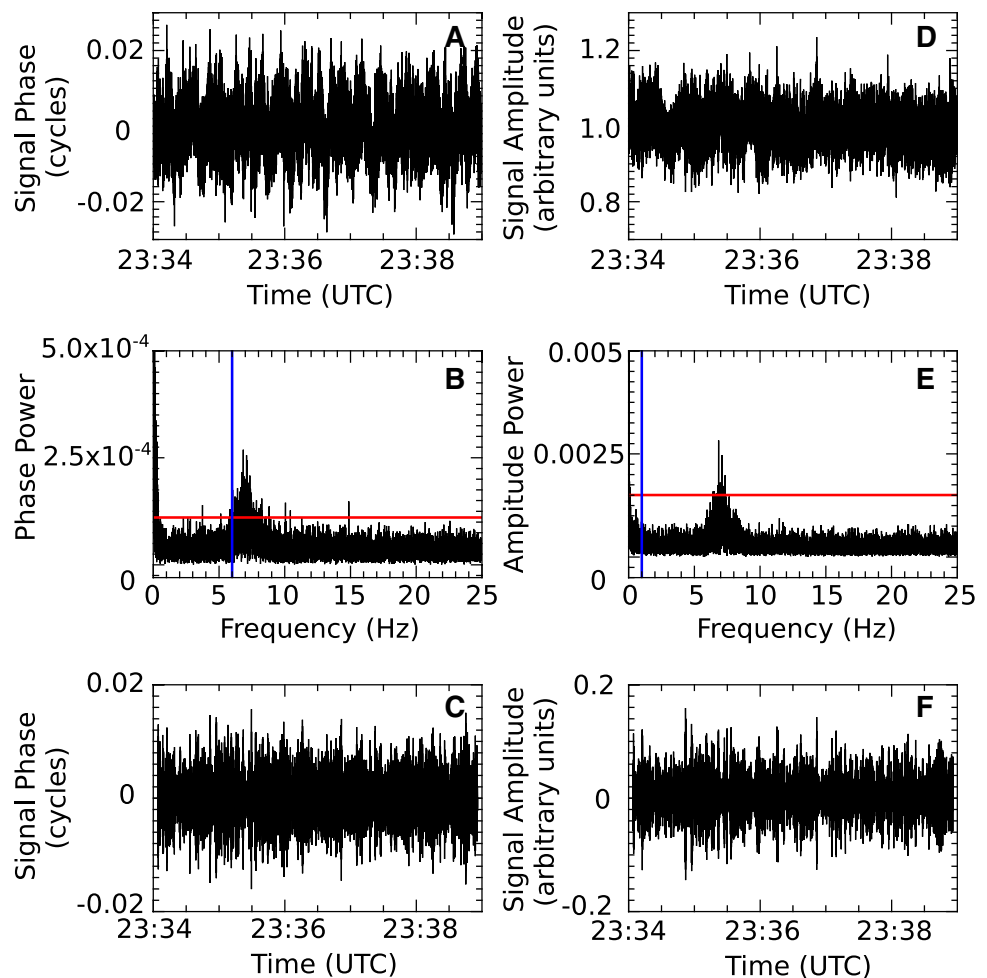


The relative Doppler–peak frequency comparison for the event observed by the NovAtel GSV4004B receiver on January 3, 2009, from 23:00 to 24:00 UTC in Cambridge Bay, outlined in Fig. 4, is shown in Fig. 6. Similar to the first example, a high correlation was observed, with correlation coefficients of 0.9948 (amplitude) and 0.9968 (phase) and with linear fits of $y = 1.024x - 0.2665$ (amplitude) and $y = 1.045x - 0.3217$ (phase).

Statistical analysis of similar peak-frequency events shows consistently high correlation coefficients above 0.9 with slopes consistently close to unity, typically within the range of 0.96–1.05.

## Discussion and conclusion

Relative Doppler between satellites, calculated by (1), not only indicates the difference between carrier waves in terms of radio frequency, but also serves as a theoretical beat frequency for interference between the two satellites. Given that the observed frequency peaks in amplitude and phase data correlate to a high degree with the relative Doppler of

the involved satellites, it is clear that these peak-frequency events involve the mutual interference of signals from distinct satellites within the GPS constellation.

Previous studies have documented instances of satellite signal interference, many of which relate to signal modulation; however, these interference events occur predominantly in geostationary systems and demonstrate little to no impact on GNSS (Bhandari and O'Keefe 2016). Within these studies, real-world observations and simulations have identified several flaws with the current L1 C/A-code modulation system (Bhandari and O'Keefe 2016).

One documented failure in signal modulation is the occurrence of cross-correlation interference—a phenomenon whereby a received strong satellite signal overpowers the acquisition of, and results in a multipath-like disruption in, a weaker signal (Qaisar and Dempster 2007; Balaei and Akos 2011). The main source of disparity in received signal strength is satellite elevation angle, where low-elevation angle satellites are received at a lower power than those of higher elevation angle (Zhu et al. 2015). The current interference events under study do not require the presence of both weak and strong signals. As seen in Fig. 3, the two

**Fig. 5** Peak frequencies (orange diamonds) for PRN 5 observed on May 11, 2015, from 06:00 to 07:00 UTC presented for amplitude and phase for receivers in both Churchill, Manitoba (**a** phase, **b** amplitude) and Fort McMurray, Alberta (**c** phase, **d** amplitude). The black line indicates the relative Doppler between PRN 5 and 20 throughout the hour, while the blue line is the relative Doppler between PRN 5 and PRN 29
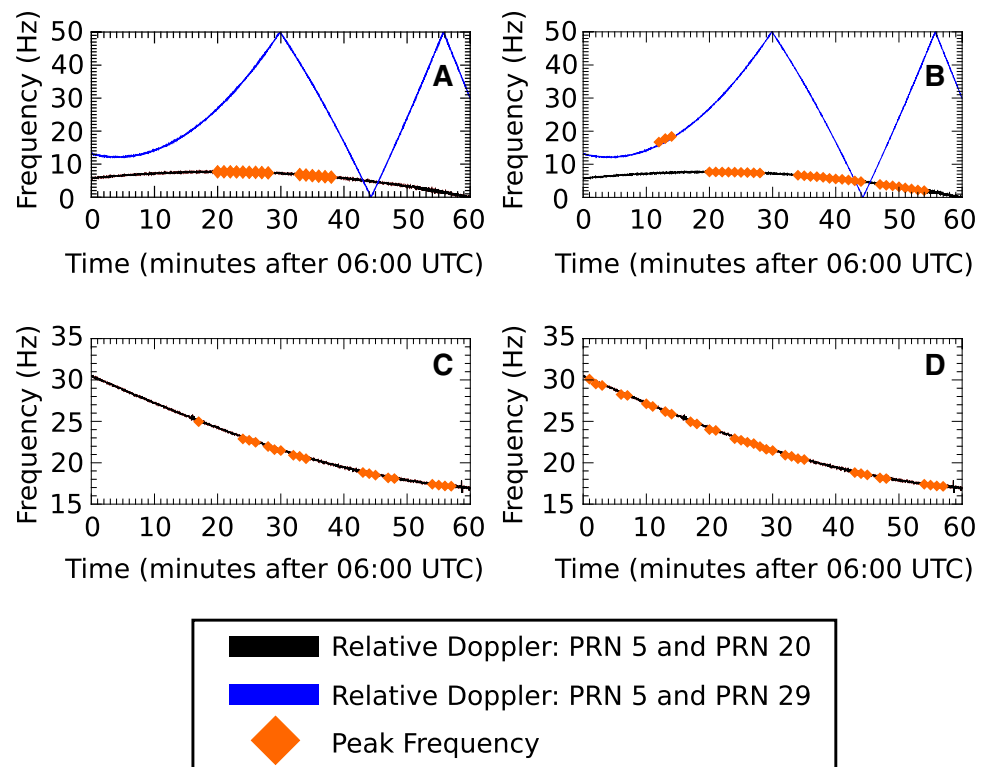
interfering satellites remain extremely close throughout the hour and, as can be expected of satellites of similar elevation angle, have nearly identical power. Analysis of other similar signal interference events has showed no evidence of a weak/strong signal requirement regardless of satellite separation distance. Given the characteristic presence of both weak and strong signals involved in cross-correlation interference, coupled with the lack of a weak/strong signal dynamic in the signal interference under study, it appears that the current interference is the result of a different interference mechanism.

Essential in the discussion of satellite signal cross-correlation is the relative Doppler of the received signals, that is, the difference in the Doppler-shifted carrier frequencies (Balaei and Akos 2011). Satellite signal cross-correlation is observed to readily occur in geostationary systems as the relative Doppler of two satellites approaches zero—an event known as Doppler collision (Zhu and Van Graas 2014; Bhandari and O'Keefe 2017). Doppler collision occurs when the relative Doppler of two satellites falls below the code loop bandwidth, which is typically 1 Hz (Bhandari and O'Keefe 2017). Cross-correlation interference is also documented to occur readily at integer multiples of 1 kHz (± 25 Hz) relative Doppler (Zhu and Van Graas 2014). The interference event presented in Fig. 5 involves relative Doppler values of 3–18 Hz (Churchill) and 17–30 Hz (Fort McMurray), both of which differ significantly from zero. Analysis of similar beat pattern events has shown no

tendency towards relative Doppler values associated with cross-correlation interference, which shows further departure between the interference events we have studied and the criteria associated with previous cross-correlation interference studies.

While common within geostationary systems, cross-correlation interference is considered rare in GNSS (Bhandari and O'Keefe 2016). The signal interference events presented here are quite common within GPS data, occurring multiple times an hour at some receivers, demonstrating yet another deviation from documented cross-correlation interference.

The mechanism by which the current signal interference occurs is not completely understood as of yet; however, it seems plausible that it is the result of code cross-correlation catalysed by the Doppler spreading of distinct satellite signals. The enhanced code cross-correlation would effectively confuse receivers, causing them to interpret the combined signal as unique to both satellites. This explanation accounts for both the involvement of specific satellites and the appearance of nearly identical beat patterns and peak frequencies in data from the involved satellites.

GPS data are used in many fields, from geodetic and space research to biological and medical studies, and in many commercial applications including navigation and transport; thus, it is extremely important that all potential impacts on the system are well understood. Sources of GPS interference such as multipath and scintillation add errors of unknown magnitude to the data obtained from GPS signals,
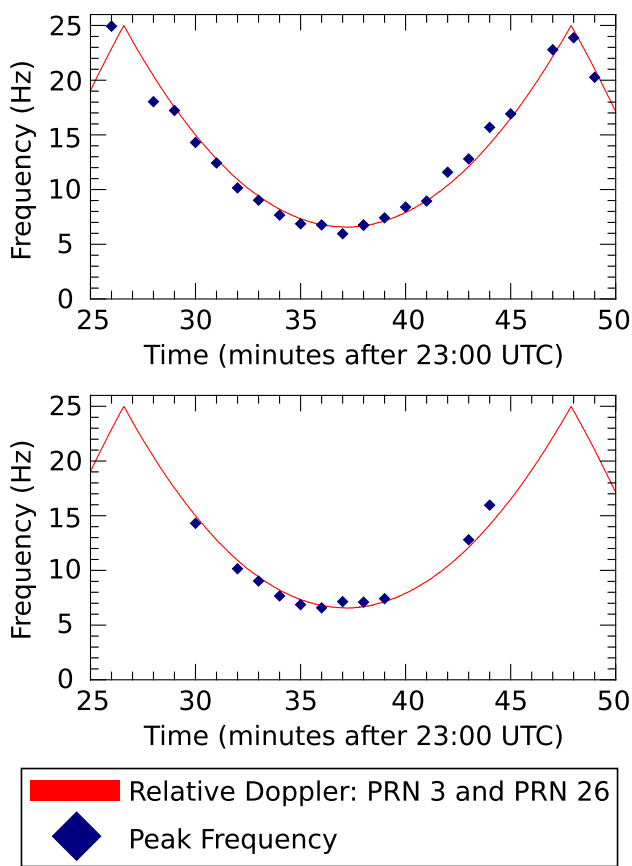
**Fig. 6** Peak frequencies (blue diamonds) for PRN 3 observed on January 3, 2009, within 23:00 to 24:00 UTC presented for amplitude (top) and phase (bottom) for the receiver in Cambridge Bay, Nunavut. The red line indicates the relative Doppler between PRN 3 and 26, aliased down to a 25 Hz range

which limits the efficacy of the information that can be derived from such signals.

Not only can signal interference contaminate results, but it can also pose serious threats to previous and ongoing research on GPS interference. Scintillation research is a popular topic, studied by many research groups throughout the world. Given the seemingly undocumented nature of the interference events we have studied, it is possible that the manifestation of this interference in amplitude and phase data could be mistaken for other phenomena, like scintillation. Not only does the sporadic beat-like pattern of this interference (Fig. 2) look similar to previously documented scintillation events in amplitude and phase (Jayachandran et al. 2017), but the interference events can have S4 and $\sigma_\varphi$ scintillation parameter values greater than 0.1—thresholds commonly used to identify scintillation (Pan and Yin 2014). We can be certain that the current interference, which can repeat daily, is not scintillation as the latter is random in nature. The signal interference outlined above may also appear to mimic multipath in some respects. In some cases,

the interference has been observed to occur sequentially, day after day, similar to the sidereal offset observed with stationary multipath. Like scintillation, multipath is also of interest in modern research, with applications in monitoring local snow depth and soil moisture content (Larson et al. 2008, 2009), for example. We can be certain that the current interference is not multipath as peak frequencies are observed on multiple spatially separated receivers at the same time, ruling out any potential station-specific obstruction.

The most prominent use for GPS is providing real-time navigation for both civilian and military use. Interference places unwanted constraints on the accuracy and precision of navigation data and is thus considered undesirable. Considerable research has gone, and continues to go, into mitigating previously identified interference events such as scintillation and multipath. With that in mind, it seems unlikely that current receivers are immune to the signal interference outlined above, especially given the multitude of identified events. Even though GPS devices typically sample in the sub–10 Hz range and not in the 50–100 Hz range, the occurrence of frequency peaks near zero Hz indicates that these devices are likely able to observe this type of interference. Given the observed errors in amplitude and phase, it is possible that errors exist in other observables like pseudorange, which has the potential to cause errors in many GPS applications.

While previous studies into GPS signal interference have identified possible cross-correlation interference, the interference events presented here depart from cross-correlation interference criteria in that they do not follow a weak/strong signal dynamic, they do not appear to be restricted to any specific relative Doppler value, and they occur frequently within GPS data. This new Doppler-mediated cross-correlation interference poses a potential threat to both scientific research, in that it can mimic both scintillation and multipath, and GPS positioning, given that it distorts both received amplitude and phase. Further studies are required to better develop the current understanding of this interference and to quantify the errors involved with it. With the development and refinement of new interference mitigation techniques, it is likely that the reduction of said interference will lead to improved data efficacy for applications involving GPS data.

## Compliance with ethical standards

**Conflict of interest** The authors declare that they have no conflict of interest.

# References

Balaei AT, Akos DM (2011) Cross correlation impacts and observations in GNSS receivers. Navig J Inst Navig 58(4):323–333

Bhandari V, O'Keefe K (2016) What is Doppler collision and is it a problem in GNSS? Inside GNSS 11(1):26–36

Bhandari V, O'Keefe K (2017) Characterization of Doppler collision and its impact on carrier phase ambiguity resolution using geostationary satellites. GPS Solut 21(4):1707–1720

Budden KG (1985) The propagation of radio waves: the theory of radio waves of low power in the ionosphere and magnetosphere. Cambridge University Press, Cambridge

Crane RK (1977) Ionospheric scintillation. Proc IEEE 65(2):180–199

Daubechies I (1990) The wavelet transform, time-frequency localization and signal analysis. IEEE Trans Inf Theory 36(5):961–1005

Doherty PH, Delay SH, Valladares CE, Klobuchar JA (2003) Ionospheric scintillation effects on GPS in the equatorial and auroral regions. Navig J Inst Navig 50(4):235–245

Fremouw EJ, Leadabrand RL, Livingston RC, Cousins MD, Rino CL, Fair BC, Long RA (1978) Early results from the DNA wideband satellite experiment—complex-signal scintillation. Radio Sci 13(1):167–187

Gold R (1967) Optimal binary sequences for spread spectrum multiplexing. IEEE Trans Inf Theory 13(4):619–621

Jayachandran PT et al (2009) Canadian high arctic ionospheric network (CHAIN). Radio Sci 44(1):1–10. https://doi.org/10.1029/2008RS004046

Jayachandran PT, Hamza AM, Hosokawa K, Mezaoui H, Shiokawa K (2017) GPS amplitude and phase scintillation associated with polar cap auroral forms. J Atmos Sol Terr Phys 164:185–191

Langley RB (1996) Propagation of the GPS signals. In: Teunissen PJG, Kleusberg A (eds) GPS for geodesy, vol 60. Lecture notes in earth science. Springer, Berlin, pp 103–140

Larson KM, Small EE, Gutmann E, Bilich A, Axelrad P, Braun J (2008) Using GPS multipath to measure soil moisture fluctuations: initial results. GPS Solut 12(3):173–177

Larson KM, Gutmann ED, Zavorotny VU, Braun JJ, Williams MW, Nievinski FG (2009) Can we measure snow depth with GPS receivers? Geophys Res Lett 36(17):1–5

McCaffrey AM, Jayachandran PT (2017) Observation of subsecond variations in auroral region total electron content using 100 Hz sampling of GPS observables. J Geophys Res Space Phys 122(6):6892–6900

Pan L, Yin P (2014) Analysis of polar ionospheric scintillation characteristics based on GPS data. In: China satellite navigation conference 2014 proceedings, vol 1. Springer, pp 11–18

Qaisar SU, Dempster AG (2007) An analysis of L1-C/A cross correlation & acquisition effort in weak signal environments. In: IGNSS symposium, Sydney, Australia, December 4–6, paper 107

Ragheb AE, Clarke PJ, Edwards SJ (2007) GPS sidereal filtering: coordinate- and carrier-phase-level strategies. J Geod 81(5):325–335

SBAS-IONO Working Group (2012) Ionospheric scintillations: how irregularities in electron density perturb satellite navigation systems. GPS World 23(4):44–50

Simsky A, Boon F (2003) Carrier phase and Doppler-based algorithms for real-time standalone positioning. In: Proceedings of GNSS, the European navigation conference, Graz, Austria, April 22–25, pp 1–25

Soubielle J, Fijalkow I, Duvaut P, Bibaut A (2002) GPS positioning in a multipath environment. IEEE Trans Signal Process 50(1):141–150

Spilker JJ Jr (1996) GPS signal structure and theoretical performance. In: Parkinson BW, Spiker JJ Jr et al (eds) Global positioning system: theory and applications, vol 1. American Institute of Aeronautics and Astronautics, Washington, DC, pp 57–80

Tamazin M, Noureldin A, Korenberg MJ, Kamel AM (2016) A new high-resolution GPS multipath mitigation technique using fast orthogonal search. J Navig 69(4):794–814

Van Dierendonck AJ, Arbesser-Rastburg B (2004) Measuring ionospheric scintillation in the equatorial region over Africa, including measurements from SBAS geostationary satellite signals. In: Proc. ION GNSS 2004, Institute of Navigation, Long Beach, California, USA, September 21–24, pp 316–324

Wernik AW, Secan JA, Fremouw EJ (2003) Ionospheric irregularities and scintillation. Adv Space Res 31(4):971–981

Zhu Z, Van Graas F (2014) Implications of C/A code cross correlation on GPS and GBAS. In: 2014 IEEE/ION position, location and navigation symposium, Monterey, CA, May 5–8, pp 282–293

Zhu Z, Van Graas F, Pelgrum W (2015) C/A code cross-correlation at a high Doppler offset. IEEE Trans Aerosp Electron Syst 51(3):1826–1838

**Connor D. Flynn** is a fourth-year undergraduate student at the University of New Brunswick working towards his B.Sc. in biology and chemistry. He has spent the last three summers working in the Department of Physics at the University of New Brunswick, focusing on the study of frequency irregularities in high-rate high-latitude GPS data.
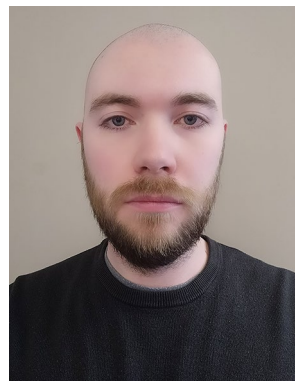
**Anthony M. McCaffrey** is senior scientific software developer in the Department of Physics at the University of New Brunswick, where he received his M.Sc. and Ph.D. in physics. His work involves writing user software for ionospheric modelling. His research focuses on the analysis of high-rate Global Positioning System observables for the purpose of ionospheric study.

**Dr. P. T. Jayachandran** is a professor of physics and chair at the University of New Brunswick. His research focuses on the physics of solar-terrestrial interactions and development of radio remote sensing techniques. He is the principal investigator of the Canadian High Arctic Ionospheric Network (CHAIN), a ground-based network of GPS receivers and Canadian Advanced Digital Ionosondes deployed in the Canadian Arctic.

**Richard B. Langley** is a professor in the Department of Geodesy and Geomatics Engineering at the University of New Brunswick, where he has been teaching and conducting research since 1981. He has a B.Sc. in applied physics from the University of Waterloo and a Ph.D. in experimental space science from York University, Toronto. Prof. Langley has been active in the development of GNSS error models since the early 1980s and has been a contributing editor and columnist for GPS World magazine since its inception in 1990. He is a fellow of the Institute of Navigation (ION), the Royal Institute of Navigation, and the International Association of Geodesy. He was a co-recipient of the ION Burka Award for 2003 and received the ION Johannes Kepler Award in 2007.